ISBN: 978-3-95450-227-1 ISSN: 2673-5490 doi:10.18429/JACoW-IPAC2022-MOPOTK034

ENERGY RAMPING PROCESS FOR SPS-II BOOSTER*

S. Jummunt†, T. Pulampong, P. Sudmuang, P. Klysubun, S. Klinkhieo
Synchrotron Light Research Institute, Muang District, Nakhon Ratchasima, Thailand

Abstract

In order to provide synchrotron light with higher photon energy and more brilliant synchrotron light than that of the existing Siam Photon Source (SPS) machine, the possibility of constructing the new 3 GeV SPS-II has been proposed. For SPS-II, the synchrotron source with in-tunnel booster is a good candidate. The booster synchrotron has been designed in order to accelerate an electron beam of 150 MeV to 3 GeV before extracted to storage ring. For a clean injection in top-up operation, the aim in the design of the booster is to achieve the electron beam with a small emittance less than 10 nm-rad and to obtain a large dynamic aperture. The energy ramping process and related effects during the energy ramp are discussed in this paper.

INTRODUCTION

The existing machine of Siam Photon Source (SPS) in Thailand is a dedicated 1.2 GeV synchrotron radiation source. It has been in operation for synchrotron radiation users since 2003. There are several experimental techniques available for Thai and international users in many fields of scientific research and industrial development. In order to provide synchrotron light with higher photon energy and more brilliant synchrotron light than that of the existing machine, the new light source (SPS-II) is in process of the consideration of construction. The SPS-II project is located in the Eastern Economic Corridor of Innovation (EECi), in the Rayong province in Thailand.

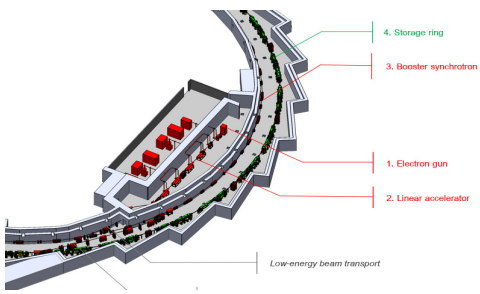

Figure 1: Layout of SPS-II source.

At present, the SPS-II source is in the process of being designed. The storage ring of SPS-II with the circumference of 327.502 m is a Double Triple Bend Achromat (DTBA) lattice, which not only obtains a beam emittance below 1 nm-rad, but also provides the sufficient spaces for the insertion devices [1]. An injector mainly consists of a 150 MeV linac as pre-injector and a 3.0 GeV booster synchrotron. The layout of SPS-II booster is shown in Fig. 1.

* Work supported by Synchrotron Light Research Institute, Thailand
† siriwan@slri.or.th

In this paper, the booster requirement, lattice consideration, the energy ramping process and related effects during the energy ramp from 150 MeV to 3 GeV are described.

BOOSTER REQUIREMENT

An RF frequency is one of the main parameters used to consider the booster circumference. The main RF frequency for SPS-II booster and storage ring was selected at a low-frequency range of 119 MHz on account of having a high RF acceptance. With the RF frequency of 119 MHz and a harmonic of 121, the total circumference is 304.829 m and the average distance between the booster and the storage ring is about 3.6 m. This distance could be suitable to mitigate the stray fields from booster magnets, and comfortable for equipment installation and transportation. To minimize stray field, our choice for the booster bending magnet is an H-type dipole. The space between STR and BS should be comfortable and enough for equipment installation and transportation.

For SPS-II storage ring, the target of beam current will be stored at 300 mA. Uniform fill with the ion-clearing gap of about 20% is a good candidate. The bucket is filled only 104 bunches (from 130 bunches) or 3.27 nC charge in each top-up cycle. With the kicker flat top width of 500 ns, the number of 52 bunches is injected bunches from linac. The required maximum bunch charge delivered to the booster from the linac should not be less than 3.3 nC for compensating the transmission efficiency of 50%. Thus, the possibility to obtain beam current provided in booster is 3.25 mA maximum. That is enough to obtain our target of 2 mA beam current for booster operation. An electron beam energy will be ramped from 150 MeV to 3 GeV with a repetition rate of 2 Hz.

LATTICE CONSIDERATION

Since the FODO lattice with combined function magnets is suitable to achieve a low-emittance beam [2], it is a good candidate for SPS-II booster synchrotron. The main advantages of combined function magnet not only can be used in limited space but also provides low-cost magnet. There are two types of combined function magnets, one is the combined dipole magnet (BD), and the other one is the combined quadrupole magnet (QF) that includes focusing quadrupole and sextupole fields. For the BD magnets, the terms of dipole field, defocusing quadrupole field, and the defocusing sextupole field are combined. The magnetic field of dipole should be about 1.0 Tesla, which can alleviate concerns of dipole magnet design. The magnetic field of about 1.0 Tesla can be achieved with the magnet length of 1.5 m and bending angle of 9 degree. The bending radius of 9.55 m can be obtained. Therefore, the 40 number of combined function dipole magnets can meet our

ISBN: 978-3-95450-227-1 ISSN: 2673-5490 doi:10.18429/JACoW-IPAC2022-MOPOTK034

requirement. The embedded defocusing quadrupoles and sextupoles in the combined function magnets can be used to correct optic function and chromaticities. respectively.

A total circumference of the booster is 304.829 m. There are 8-fold symmetric lattices, and each symmetric lattice consists of 5 cells of FODO lattice (Fig. 2). There are no dispersion-free straight sections provided. The low beam emittance of 5.87 nm-rad can be achieved to provide the high injection efficiency for top-up operation [3]. The main parameters of SPS-II booster are listed in Table 1.

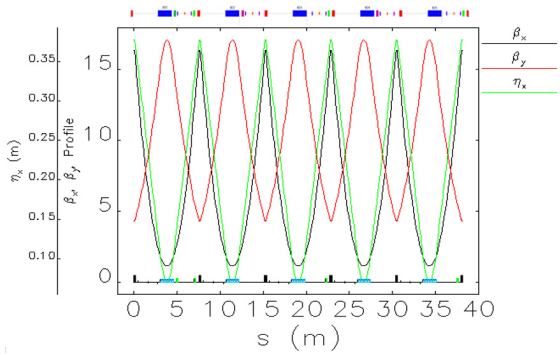

Figure 2: Optical functions for one symmetric lattice.

Table 1: The Main Parameters of the SPS-II Booster

Parameters	Booster synchrotron
Circumference	304.829 m
Beam energy	3.0 GeV
Relativistic factor (γ)	5870.85
Emittance	5.87 nm-rad
Nat. energy spread	0.091 %
Nat. chromaticity (ξ_x/ξ_y)	-23.63/ -10.31
Tune (Q_x/Q_y)	14.71/5.61
Momentum compaction (α_c)	1.674e-3
Energy loss per turn (U_0)	0.75 MeV
RF frequency	119.00 MHz
Harmonic number	121
Beam current	2 mA
Repetition rate	2 Hz

All the booster dipole magnets with the required effective length of 1.5 m are the maximum field of 1.048T, quadrupole gradient of 3.158 T/m and sextupole component of 16.03 T/m^2. Each component cannot be separately controlled. Quadrupoles have 2 families. The first one is the combined function quadrupole with the field gradient of 19.474 T/m and 64.044 T/m^2 for quadrupole and sextupole terms, respectively. The effective length provided is 0.25 m. Other one is the defocusing quadrupole with a small gradient of only 0.5 T/m and the length of 0.2 m. For sextupole magnets, there are two families with the required gradient of 750 T/m^2 and 300 T/m^2 for focusing and defocusing sextupoles, respectively while the required effective length is 0.2 m. The expected good field region, where the quadrupole gradient error is below 5×10^{-4}, is ±20 mm for all magnets. The magnet prototypes are in the process of design.

ENERGY RAMPING PROCESS

At the nominal tune of 14.72/5.61, not only low-emittance beam and large dynamic aperture can be achieved but also the momentum acceptance obtained is higher than 2%. The synchrotron radiation loss in booster is 0.75 MeV/turn from dipole magnets. For booster, the overvoltage (eV/U_0) higher than 1.5 is desired. Thus, the RF voltage for the booster is only 1.2 MV required with the purpose of providing 1.7% RF acceptance. With the half-period injection, the booster should provide enough energy to the beam withing 0.25 second for the repetition rate of 2 Hz. Figure 3 shows the ramping pattern of energy ramping and RF cavity voltage.

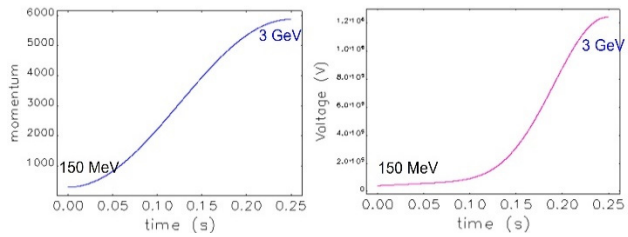

Figure 3: Beam momentum and generated RF voltage patterns in the booster during energy ramping.

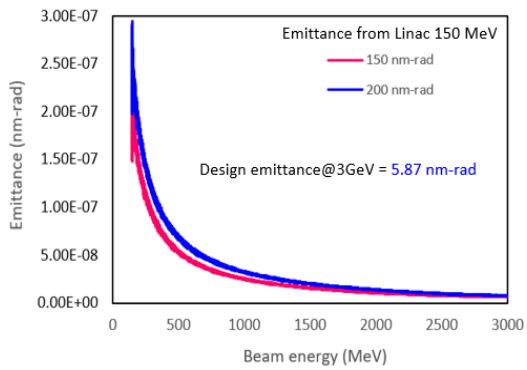

Figure 4: Horizontal emittance evolution during energy ramping in the booster.

Figure 4 shows the beam emittance variation during the energy ramping performed by using Elegant code [4]. It is noticeable that during the early stage of the energy ramping the beam parameters show large fluctuation. At the end of the ramping process, the horizontal beam emittance is about 6.45 nm-rad and 7.66 nm-rad for the case of the 150 MeV beam injected from linac with 150 nm-rad and 200 nm-rad emittances, respectively. The results are slightly larger than that from the twiss parameter at about 5.9 nm-rad. However, the emittance below 10 nm-rad is still workable for beam injection into the storage ring. After the ramping process, the beam at the energy of 3 GeV will be extracted to transfer line before going to Storage ring.

EDDY CURRENT EFFECT

During ramping energy, eddy currents can be generated in the vacuum chamber of the bending because of the time dependent fields. The most important multipole field produced is the sextupole component. The generated

ISBN: 978-3-95450-227-1 ISSN: 2673-5490 doi:10.18429/JACoW-IPAC2022-MOPOTK034

sextupole strength leads to the change in chromaticity, which would result in the dynamic aperture reduction. A sinusoidal energy ramping has been assumed for this calculation as shown in Fig. 3. The sextupole strength induced by eddy current can be calculated using the in Eq. (1) shown below [5]:

$$m = \frac{1}{2B\rho}\frac{\partial^2 B}{\partial x^2} = \frac{\mu_0 \delta e}{h\rho}\frac{2\pi f \sin(2\pi f t)}{\alpha - \cos(2\pi f t)} J(h/a) \quad (1)$$

where J*(h/a)* is given by $\int_0^1 \left[x^2 + \left(\frac{h}{a}\right)^2 (1-x^2)\right]^{1/2} dx$

μ_0 is the vacuum permeability, $4\pi\times10^{-7}$
σ is the conductivity of stainless-steel vacuum chamber, $1.3\times10^6\ \Omega^{-1}m^{-1}$
a is the vacuum chamber half-width
h is the vacuum chamber half-height
ρ is the radius of bending magnet
e is the chamber thickness

For the SPS-II booster, a half-vacuum chamber in bending magnet is 10 mm with round shape. To minimize the eddy current, stainless steel used would be less than 1 mm thickness. It is noticed that the sextupole strength also depends on the repetition rate of booster operation. The induced sextupole strength was estimated as a function of time with assuming sinusoidal energy ramp. Comparison of sextupole strength induced during the ramping energy between the repeitition of 2 Hz and 3 Hz is plotted in Fig. 5. The sextupole strength for the case of 2 Hz repetition rate is lower than that of the case of 3 Hz. The reason to choose the repetition rate of 2 Hz is to avoid an additional chromaticities occurring during the ramp and to guarantee reliable machine operation.

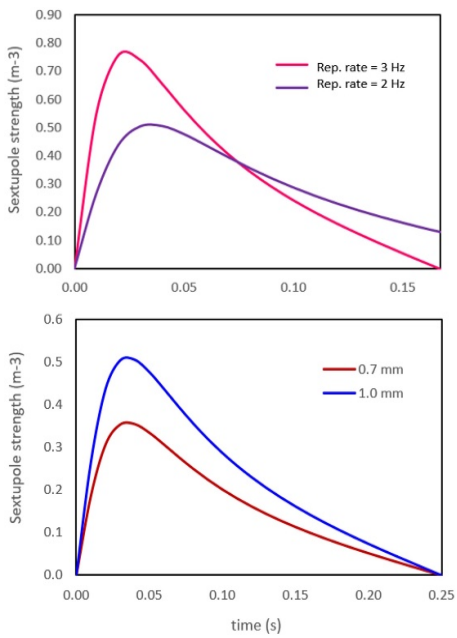

Figure 5: (top) Sextupole strength induced by eddy current for the repetition rate of 2 Hz and 3 Hz and (bottom) the sextupole strength varying the vacuum thickness of 0.7 mm and 1 mm at the repetition rate of 2 Hz.

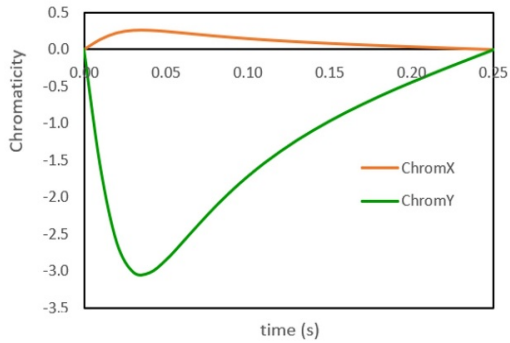

Figure 6: Eddy current induced chromaticity change.

In SPS-II booster, the largest sextupole strength induced by eddy current is 0.506 m^{-3} reached at 35 msec. Figure 6 shows dependence of the chromaticity changes due to the eddy current as a function of time. In the SPS-II booster, the embedded sextupole components in bending and focusing quadrupole magnets have been used for correcting the natural chromaticity. However, the induced sextupole components will lead to change the chromaticity during the ramping process. This chromaticity change can be corrected close to the target by adjusting magnetic field of two extra separate sets of focusing and defocusing sextupoles. Therefore, we can keep the chromaticity in ramping up process.

SUMMARY

For SPS-II, a full energy booster sharing the same tunnel with the storage ring has been designed. A low emittance is achieved allowing a high efficiency for a clean injection in top-up operation. The energy ramping process and related effects during the energy ramp have been studied. In order to avoid an additional chromaticities occurring during the ramp and to guarantee reliable machine operation, the repetition rate of 2 Hz is a good selection. The schematics for injection and extraction beam are in process of consideration.

REFERENCES

[1] P. Klysubun, T. Pulampong, and P. Sudmuang, "Design and optimisation of SPS-II storage ring", in *Proc. 8th Int. Particle Accelerator Conf. (IPAC'17)*, Copenhagen, Denmark, May 2017, pp. 2773-2775. doi:10.18429/JACoW-IPAC2017-WEPAB086

[2] L. Liu, X. R. Resende and A. R. D. Rodrigues, F. H. Sá, "A new booster synchrotron for the Sirius project", in *Proc. 5th Int. Particle Accelerator Conf. (IPAC'14)*, Dresden, Germany, Jun 2014, pp. 1959-1961. doi:10.18429/JACoW-IPAC2014-WEPRO009

[3] S. Krainara, T. Pulampong, P. Sudmuang, P. Klysubun, and S. Klinkhieo, "Conceptual design of booster synchrotron for Siam Photon Source II", in *Proc. 12th Int. Particle Accelerator Conf. (IPAC'21)*, Campinas, SP, Brazil, May 2021, pp. 2795-2797. doi:10.18429/JACoW-IPAC2021-WEPAB089

[4] M. Borland, "elegant: A Flexible SDDS-Compliant Code for Accelerator Simulation," Advanced Photon Source Light Source Note LS-287, 2000. https://doi.org/10.2172/761286

ISBN: 978-3-95450-227-1 ISSN: 2673-5490 doi:10.18429/JACoW-IPAC2022-MOPOTK034

[5] Y.M. Peng, J.Y. Li, C. Meng, and H.S. Xu, "Study of the ramping process for HEPS booster", in *Proc. 10th Int. Particle Accelerator Conf. (IPAC'19)*, Melbourne, Australia, May 2019, pp. 1521-1523. doi:10.18429/JACoW-IPAC2019-TUPGW052